ATMOSMJ: REVISITING GATING MECHANISM FOR AI WEATHER FORECASTING BEYOND THE YEAR SCALE

A PREPRINT

Minjong Cheon

jmj2316@kaist.ac.kr

Korea Advanced Institute of Science and Technology

ABSTRACT

The advent of Large Weather Models (LWMs) has marked a turning point in data-driven forecasting, with many models now outperforming traditional numerical systems in the medium range. However, achieving stable, long-range autoregressive forecasts beyond a few weeks remains a significant challenge. Prevailing state-of-the-art models that achieve year-long stability, such as SFNO and DLWP-HPX, have relied on transforming input data onto non-standard spatial domains like spherical harmonics or HEALPix meshes. This has led to the prevailing assumption that such representations are necessary to enforce physical consistency and long-term stability. This paper challenges that assumption by investigating whether comparable long-range performance can be achieved on the standard latitude-longitude grid. We introduce AtmosMJ, a deep convolutional network that operates directly on ERA5 data without any spherical remapping. The model's stability is enabled by a novel Gated Residual Fusion (GRF) mechanism, which adaptively moderates feature updates to prevent error accumulation over long recursive simulations. Our results demonstrate that AtmosMJ produces stable and physically plausible forecasts for about 500 days. In quantitative evaluations, it achieves competitive 10-day forecast accuracy against models like Pangu-Weather and GraphCast, all while requiring a remarkably low training budget of 5.7 days on a V100 GPU. Our findings suggest that efficient architectural design, rather than non-standard data representation, can be the key to unlocking stable and computationally efficient long-range weather prediction.

Keywords Convolutional Neural Network (CNN) · ERA5 Reanalysis Data · Global Weather Forecasting · Gated Residual Fusion (GRF) · InceptionNeXt

1 Introduction

The accelerating impacts of climate change have stimulated a growing interest in data-driven weather prediction models, leading to the emergence of so-called *Large Weather Models (LWMs)* Chempan and contributors [2024]. These models leverage advances in artificial intelligence to provide efficient alternatives to traditional numerical weather prediction systems. Recent models such as Huawei's Pangu-Weather Bi et al. [2023], Google's GraphCast Lam et al. [2022], NeurlGCM Kochkov et al. [2023] NVIDIA's FourCastNet Pathak et al. [2022], Alibaba's Fuxi-Weather Chen et al. [2023], Microsoft's Stormer Nguyen et al. [2023], and ArchesWeather Couairon et al. [2024a] have all demonstrated impressive performance in medium-range forecasting (up to 10 days), surpassing high-resolution forecasts of operational systems such as ECMWF's HRES model in accuracy. Moreover, Fuxi's seasonal-to-seasonal (S2S) variant has recently shown skill beyond ECMWF's S2S model, marking a significant milestone in long-range AI-based forecasting Chen et al. [2024].

Despite recent advances, most AI-based weather models remain confined to the medium range. Stable autoregressive prediction over extended periods, such as year-long forecasts, remains a challenging and underexplored frontier. According to Karlbauer et al.'s paper, GraphCast's performance begins to degrade after approximately 1.5 months, while Pangu-Weather exhibits significant drift over time, producing unrealistic outputs beyond 5 months—even when

solar radiation is used as an external forcing. These limitations demonstrate that current models, although powerful in the medium range, struggle to maintain stability and physical realism in the long term. Achieving robust long-term simulations, which are crucial for climate modeling and analysis, necessitates stable and physically consistent backbone models Karlbauer et al. [2024]. Only a few recent efforts have demonstrated promising long-term results by leveraging specialized architectural designs or data representations.

For instance, the Spherical Fourier Neural Operator (SFNO) stands out as a backbone for stable long-term climate simulations. SFNO learns a spectral representation of global weather data via spherical harmonics, inherently respecting the Earth's geometry and significantly enhancing long-range stability. This representation enables efficient spatial information exchange and supports physically consistent autoregressive forecasting. Notably, the AI2 Climate Emulator (ACE) family—such as ACE, ACE2, and ACE2-SOM—builds upon SFNO to achieve stable climate modeling. These models exhibit multi-decadal to millennial stability **???**. Another example is the HEALPix-based approach developed by Karlbauer et al., known as DLWP-HPX (Deep Learning Weather Prediction - HEALPix). This model employs a parsimonious deep learning architecture on a Hierarchical Equal Area isoLatitude Pixelation (HEALPix) mesh to forecast a subset of atmospheric variables. It provides stable autoregressive rollouts beyond one year by utilizing the equal-area pixelation and hierarchical structure of the grid. Extending this idea, DLESyM is another HEALPix-based model that achieves millennial-scale climate simulations with minimal drift and strong performance on key variability metrics **?**.

However, recent models such as ArchesWeather Couairon et al. [2024a] and Microsoft's Stormer Nguyen et al. [2023] have demonstrated that well-designed yet relatively simple architectures can achieve state-of-the-art performance in medium-range forecasting. Although these models do not explicitly target long-term prediction, their success raises an important question: *Is it truly necessary to transform ERA5 into alternative spatial domains to achieve stable long-range forecasts?* Rather than relying on spherical harmonics or HEALPix grids, we investigate whether comparable or even better stability can be attained using novel deep learning architectures trained directly on the standard grid. To this end, we propose a novel gating mechanism called Gated Residual Fusion (GRF), aiming to achieve long-term prediction by isolating the impact of architectural innovations from that of spatial domain representations.

Our key contributions are summarized as follows:

- Our study systematically evaluates autoregressive forecasting performance using models trained directly on the standard latitude–longitude grid, without reliance on spherical or spectral transformations.
- We demonstrate that our proposed module, Gated Residual Fusion (GRF) can provide competitive long-range stability.
- Notably, AtmosMJ matches the performance of other existing state-of-the-art (SOTA) models while requiring a remarkably low computational budget of 5.7 days on a V100 GPU. Trained and evaluated at 1.5° resolution, it also demonstrates exceptional inference efficiency by generating a 500-day forecast in approximately 21 seconds.

2 Related Works

2.1 Overarching Developments in Global Medium-Range Forecasting

The consistent demonstration across models like FourCastNet, Pangu-Weather, and GraphCast of being orders of magnitude faster while maintaining comparable or superior accuracy to state-of-the-art NWP systems (IFS/HRES) signifies a fundamental resolution of the long-standing speed-accuracy trade-off in medium-range forecasting Lam et al. [2022]Bi et al. [2023]Pathak et al. [2022]. This is not merely an incremental improvement but a transformative shift, where architectural innovations in deep learning—such as Adaptive Fourier Neural Operators, Graph Neural Networks, and various Transformer adaptations—enable this unprecedented efficiency. The implication is that deep learning is moving beyond a supplementary role to becoming a primary, transformative force in operational weather forecasting, making advanced predictions more accessible and timely. The architectural landscape of global medium-range deep learning weather models reveals a clear convergence towards Transformer architectures, albeit with crucial domain-specific adaptations. Models such as ClimaX, Pangu-Weather, Stormer, and ArchesWeather all leverage variants of the Transformer. However, the success of these models is not solely due to the generic attention mechanism but also to how they are tailored for meteorological data. Examples include ClimaX's innovative variable tokenization and aggregation , Pangu-Weather's 3D Earth Specific Transformer , and ArchesWeather's Cross-Level Attention for vertical interactions. Other successful architectures, such as Graph Neural Networks (GraphCast) and Fourier Neural Operators (FourCastNet) , also demonstrate the power of specialized designs. This indicates that while the general attention mechanism is powerful for capturing long-range dependencies, the specific inductive biases and adaptations for Earth's

spherical geometry, multi-variable interactions, and vertical atmospheric levels are crucial for achieving state-of-the-art performance, leading to a nuanced and evolving architectural landscape Couairon et al. [2024a]Bi et al. [2023]**?**.

2.2 Overarching Developments in Longer Simulation Models

The models designed for longer simulations, such as SFNO and DLWP-HPX, collectively demonstrate a significant leap in the field of climate modeling by prioritizing long-term stability and computational efficiency. SFNO's spherical Neural Operator architecture is crucial for maintaining physical plausibility and achieving remarkable autoregressive stability over extended periods, including full-year rollouts, by respecting Earth's geometry and symmetries. This design choice ensures that the model's internal representation and dynamics remain physically consistent, even over thousands of sequential time steps, which is vital for reliable climate projections. Furthermore, SFNO models trained with higher effective resolutions exhibit greater ensemble dispersion, a beneficial characteristic for achieving well-calibrated probabilistic forecasts, although long-lead time fine-tuning can sometimes reduce ensemble spread Bonev et al. [2023]. Similarly, DLWP-HPX, despite its parsimonious design and use of coarser resolution and fewer prognostic variables compared to more complex models, achieves realistic atmospheric states that respect seasonal trends over 1-year simulations. Its utilization of the Hierarchical Equal Area isoLatitude Pixelization (HEALPix) mesh is key to its success, enabling the development of location-invariant convolution kernels that effectively propagate weather patterns globally without the need for specialized handling of polar or equatorial regions. This model's ability to maintain skill at one-week lead times, being only about one day behind state-of-the-art NWP models, highlights its efficiency and potential for sub-seasonal and seasonal forecasting. These advancements underscore a critical trend towards developing highly efficient, stable, and physically consistent AI models that can bridge the gap between short-term weather forecasting and multi-decadal climate projections, making long-term climate research more accessible and less resource-intensive Karlbauer et al. [2024].

3 Methodology

3.1 Data Description

Following the variables listed in Table 1, we utilized the European Centre for Medium-Range Weather Forecasts (ECMWF) Reanalysis v5 (ERA5) dataset, downloaded from the WeatherBench2 repository Rasp et al. [2024]. A total of 71 daily-mean atmospheric variables, aggregated from hourly data, were used. These comprised six single-level variables and five variables sampled at 13 pressure levels, extending from near the surface up to the lower stratosphere. These include essential prognostic fields such as zonal and meridional wind components, temperature, humidity, and geopotential, which are crucial to define atmospheric dynamics. In addition, orography was included as a static topographic variable. The processed dataset was represented as tensors of shape $121 \times 241 \times 71$, corresponding to a 1.5° spatial resolution. For model training and evaluation, the data was split into training (1979–2015), validation (2016–2017), and test (2018) periods.

Table 1: Overview of meteorological variables used from the ERA5 dataset, including pressure-level and single-level fields.

Variable name	**Short name**	**Vertical levels (hPa)**	**Units**
Pressure-level variables			
Geopotential	Z	1000, 925, 850, 700, 600, 500, 400, 300, 250, 200, 150, 100, 50	m^2/s^2
Temperature	T	1000, 925, 850, 700, 600, 500, 400, 300, 250, 200, 150, 100, 50	K
Specific Humidity	Q	1000, 925, 850, 700, 600, 500, 400, 300, 250, 200, 150, 100, 50	kg/kg
Zonal Wind	U	1000, 925, 850, 700, 600, 500, 400, 300, 250, 200, 150, 100, 50	m/s
Meridional Wind	V	1000, 925, 850, 700, 600, 500, 400, 300, 250, 200, 150, 100, 50	m/s
Single-level variables			
2m Temperature	T2m	-	K
Mean Sea Level Pressure	MSL	-	Pa
Surface Pressure	SP	-	Pa
Total Column Water Vapor	TCWV	-	kg/m^2
Orography	OROG	-	m
TOA Incident Solar Radiation	TISR	-	J/m^2

3.2 Architecture of AtmosMJ

Our neural network architecture is a deep convolutional model inspired by InceptionNeXt Yu et al. [2024], which itself builds upon the success of efficient convolutional architectures such as KARINA Cheon et al. [2024] and DLWP-HPX Karlbauer et al. [2024]. The input data are first processed by a stem block consisting of a depthwise separable convolution followed by layer normalization, which processes the input for multi-scale feature extraction. The main body of the network consists of four stages of InceptionNeXt blocks with Geocyclic Padding Cheon et al. [2024]. To facilitate channel-wise interaction and mitigate information loss across stages, we additionally incorporate a Gated Residual Fusion (GRF) mechanism between blocks. Since the model is designed to preserve the spatial resolution of the input throughout the entire network, no downsampling or upsampling operations are applied. Finally, a depthwise convolutional layer maps the features to the target number of output variables. The overall architecture of the InceptionNeXt and GRF is illustrated in Figure 1.

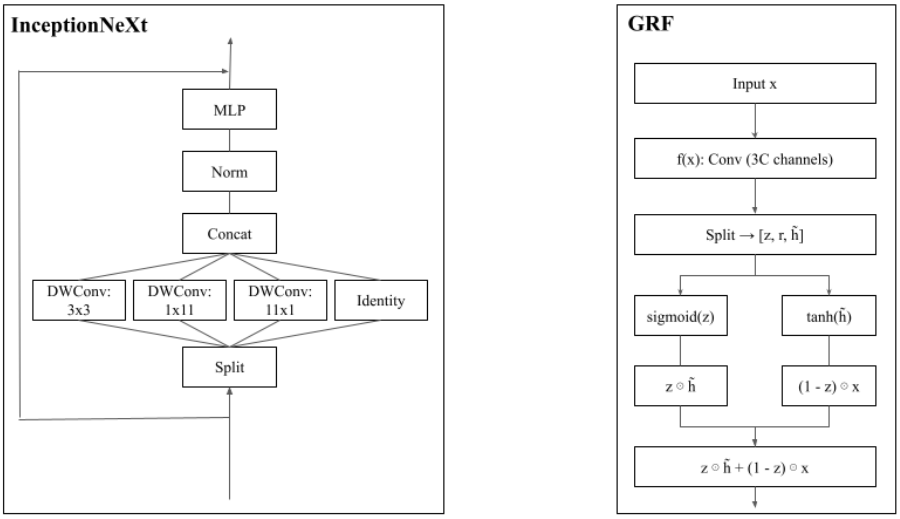

Figure 1: Main architecture of the proposed AtmosMJ model for global weather forecasting. The InceptionNeXt block (left) performs multi-scale depthwise convolution and channel mixing via MLP, while the GRF block (right) applies a gated residual fusion using update and candidate branches from a 3-way split.

3.3 Gated Residual Fusion (GRF)

Long-term autoregressive simulations require models to maintain stability over hundreds of recursive steps. To this end, we propose Gated Residual Fusion (GRF), a gating mechanism designed to mitigate error accumulation by controlling the balance between the newly transformed features and the original input. The GRF module is typically applied at the end of each network block and performs the following core operation:

$$\mathbf{y} = \mathbf{z} \odot \tilde{\mathbf{h}} + (1 - \mathbf{z}) \odot \mathbf{x}, \quad \mathbf{z} = \sigma(\mathbf{z}),\ \tilde{\mathbf{h}} = \tanh(\tilde{\mathbf{h}}),$$

where $\mathbf{x}$ is the input feature, $\tilde{\mathbf{h}}$ is the candidate update, and $\mathbf{z}$ is a learnable gate that adaptively determines the contribution of each. The gating function $\sigma(\cdot)$ denotes the element-wise sigmoid activation, ensuring that the gate values remain in the range $[0, 1]$.

This soft, element-wise fusion serves multiple purposes. First, it stabilizes gradient flow: the residual branch $(1 - \mathbf{z}) \odot \mathbf{x}$ acts as a dynamic identity shortcut, preserving a direct path for gradients and avoiding vanishing or exploding gradients during deep updates. Second, the gate $\mathbf{z}$ selectively suppresses noise and emphasizes salient signals—when $\mathbf{z}_{i,j,k,l} \approx 0$, the output retains original information; when $\mathbf{z}_{i,j,k,l} \approx 1$, it incorporates new, non-linear structure. Third, by learning unique gates at each layer, the model can perform stage-wise routing: early stages preserve large-scale structure, while deeper stages introduce finer details. This dynamic, multi-scale control enhances both short-term accuracy and long-range consistency.

Algorithm 1: Gated Residual Fusion (GRF)

Input : Input feature tensor $\mathbf{x} \in \mathbb{R}^{B\times C\times H\times W}$
Output : Fused output $\mathbf{y} \in \mathbb{R}^{B\times C\times H\times W}$

$\mathbf{h} \leftarrow f(\mathbf{x})$; `//Pointwise Conv with` $2C$ `output channels`
$[\mathbf{z}, \tilde{\mathbf{h}}] \leftarrow \text{Split}(\mathbf{h})$; `//Update, reset, candidate`
$\mathbf{z} \leftarrow \sigma(\mathbf{z})$; `//Gating with sigmoid`
$\tilde{\mathbf{h}} \leftarrow \tanh(\tilde{\mathbf{h}})$; `//Candidate transformation`
$\mathbf{y} \leftarrow \mathbf{z} \odot \tilde{\mathbf{h}} + (1 - \mathbf{z}) \odot \mathbf{x}$; `//Gated fusion (reset unused)`
return $\mathbf{y}$

Remark. *When* $\mathbf{z} \approx 0$*, the GRF behaves as an identity mapping:* $\mathbf{y} \approx \mathbf{x}$*. When* $\mathbf{z} \approx 1$*, it performs a full update:* $\mathbf{y} \approx \tilde{\mathbf{h}}$*. This dynamic control stabilizes long recursive rollouts by preventing feature drift and maintaining physical coherence. Unlike recurrent GRUs, GRF operates purely in a feedforward spatial context and introduces minimal computational overhead.*

3.4 Training Details

Recent AI-based weather prediction methods can be broadly categorized into three forecasting paradigms: *direct forecasting*, *continuous forecasting*, and *iterative forecasting*. In **direct forecasting**, the model is trained to predict the weather at a specific lead time T directly from the initial condition X_0, such that

$$X_T = f_\theta(X_0).$$

Continuous forecasting extends this approach by treating the lead time as an additional input, enabling a single model to predict multiple horizons:

$$X_T = f_\theta(X_0, T).$$

Iterative forecasting, on the other hand, predicts short-term increments δt and recursively feeds outputs back into the model to forecast longer sequences:

$$X_{t+\delta t} = f_\theta(X_t).$$

This iterative approach has been adopted by recent large weather models such as Stormer Nguyen et al. [2023], and GraphCast Lam et al. [2022], often with fine-tuning strategies that improve long-range stability over multiple rollout steps. Since our dataset consists of daily-resolution fields, we did not adopt roll-out based fine-tuning to avoid error accumulation and simplify the training pipeline. We utilized a weighted root mean squared error (RMSE) loss that incorporates latitude-based weighting over the global latitude–longitude grid.

$$A(\varphi_i) = N_{\text{lat}} \frac{\cos \varphi_i}{\sum_{l=1}^{N_{\text{lat}}} \cos \varphi_l} \tag{1}$$

where φ_i denotes the latitude (in radians) of the i-th grid point, and N_{lat} is the total number of latitude points. This formulation ensures that each latitude is weighted proportionally to the surface area it represents on the sphere.

where N_{lat} represents the number of grid points in the latitudinal direction.

The RMSE_l between ground truth (ERA5) $y_{t,i,j}$ and forecast $\hat{y}_{t,l,i,j}$ for lead time l is defined as follows:

$$\text{RMSE}_l = \sqrt{\frac{1}{N_{\text{time}} N_{\text{lat}} N_{\text{lon}}} \sum_{t=1}^{N_{\text{time}}} \sum_{i=1}^{N_{\text{lat}}} \sum_{j=1}^{N_{\text{lon}}} A(\varphi_i)(\hat{y}_{t,l,i,j} - y_{t,i,j})^2} \tag{2}$$

The hyperparameter setup utilized to train the AtmosMJ on the daily ERA5 dataset is described in Table 2. A time step (dt) of one day is used to train the model. A CosineAnnealingLR scheduler is used to gradually lower the learning rate during training, with the learning rate set at 0.001. The model incorporates and forecasts 71-channel inputs and outputs, which correspond to various atmospheric factors, and employs Z-score normalization. The model is trained over a maximum of 150 epochs, with AdamW serving as the optimizer for steady convergence. These parameters were selected to guarantee stable convergence and balanced learning dynamics over extended forecasts. Notably, training the model required only 5.7 days on a single V100 GPU.

Table 2: Training hyperparameters used for AtmosMJ on the ERA5 dataset.

Hyperparameter	**Value**
Loss	L2
Learning Rate (LR)	0.001
Scheduler	CosineAnnealingLR
dt	1 day
Number of In-Channels	71
Number of Out-Channels	71
Normalization	Z-score
Optimizer Type	AdamW
Max Epochs	150

4 Result

4.1 Impact of Gated Residual Fusion on Model Performance

As shown in Figure 2, the introduction of gating mechanisms in our InceptionNeXt-based backbone leads to a noticeable reduction in feature map variance across normalized depth. Here, normalized depth refers to the relative position of layers across different stages of the network, scaled between 0 (input) and 1 (output).

The red line, representing the network with gating, consistently exhibits significantly lower variance compared to the black line, which denotes the network without gating. Particularly in the initial stages (approx. 0.0 to 0.15 normalized depth), both configurations show a sharp drop in variance, but the gated network reaches a much lower and more stable baseline. As the network depth increases (from approximately 0.2 to 0.85 normalized depth), the variance in the network without gating (black line) gradually increases, indicating a potential for unstable activations or information diffusion in deeper layers. In contrast, the gated network (red line) maintains a remarkably low and stable variance throughout this middle range.

This suppression of variance can be interpreted as a reduction in uncertainty regarding the feature distributions, which facilitates more stable and efficient optimization by mitigating activation explosion and promoting consistent information flow throughout the network. By keeping the feature map variance in check, gating mechanisms likely contribute to a more robust learning process, preventing issues such as vanishing or exploding gradients and thereby enhancing the overall performance and trainability of deep neural networks **?**.

Furthermore, this observed stability of feature map variance strongly suggests that gating mechanisms are beneficial for data-driven weather forecasting models, especially for long-term simulations. In autoregressive models commonly used in weather forecasting, small errors can accumulate over time, leading to significant divergence in long-term predictions. By effectively controlling the variance, gating mitigates this error accumulation, ensuring a stable and consistent propagation of information across numerous prediction steps.

4.2 Quantitative evaluation against State-of-the-art models

Figure 3 compares the 10-day forecast RMSE of AtmosMJ against Pangu-Weather Bi et al. [2023], GraphCast Lam et al. [2022], and the IFS HRES operational forecast across six key meteorological variables. To ensure a fair comparison at the same spatial resolution (1.5°) as AtmosMJ, we report the deterministic scores of Pangu-Weather and GraphCast provided by WeatherBench 2. Despite being trained at higher resolutions, both models are evaluated after regridding to match the coarser scale. The results indicate that AtmosMJ achieves competitive long-range forecast accuracy, especially in upper-level variables such as Z500 and T850, maintaining lower error growth over time compared to deep learning counterparts.

Table 3 presents a quantitative comparison of recent AI-based global weather forecasting models using RMSE scores for selected variables at a 24-hour lead time. All evaluations are conducted using ERA5 data from the year 2020. The variables include geopotential at 500 hPa (Z500), temperature at 850 hPa (T850), specific humidity at 700 hPa (Q700), and wind components (U/V850), as well as near-surface temperature (T2m) Couairon et al. [2024a]. All models are either trained or evaluated at 1.5° resolution for a fair comparison.

Our model, AtmosMJ, achieves competitive performance across several key variables, showing similar or even better RMSE scores compared to more recent models such as Stormer and ArchesWeather-M. In particular, AtmosMJ records

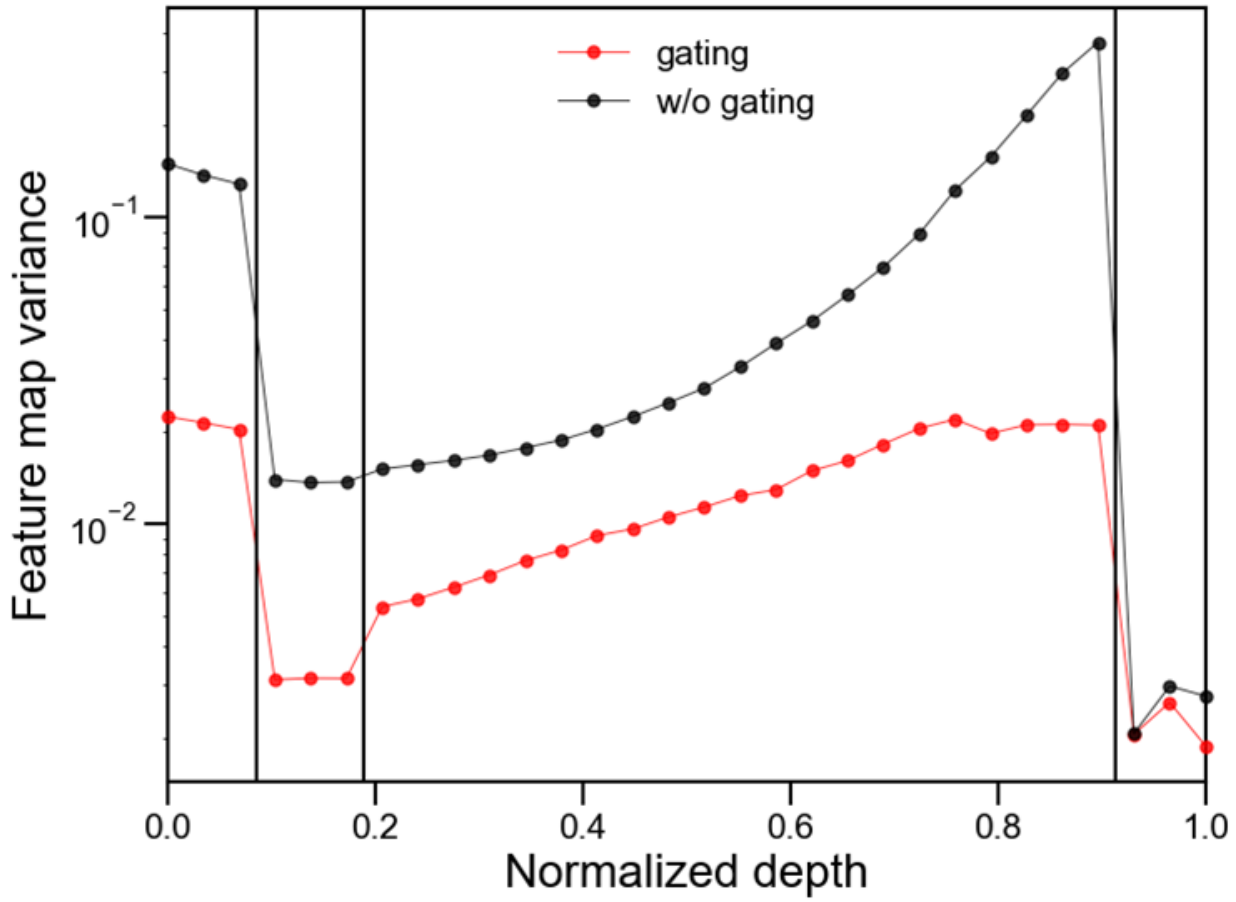

Figure 2: Comparison of feature map variance across normalized depth between models with (red) and without (black) gating. Gating mechanisms reduce activation variance, which correlates with decreased uncertainty and improved optimization dynamics.

the lowest RMSE in Q700, U850, V850, and T2m. Notably, this is achieved with the smallest reported training cost—just 5.7 V100-days—highlighting AtmosMJ's high computational efficiency relative to the other models.

Table 3: Comparison of AI weather models on RMSE scores for key weather variables with 24-hour lead time at 1.5° resolution. All models are evaluated on 2020 ERA5 data. Results for Pangu-Weather, GraphCast, and HRES are taken from the ArchesWeather paper Couairon et al. [2024a]. Cost is the training computational budget in V100-days. Best scores for each variable are in bold.

Model	Res	Cost	Z500	T850	Q700	U850	V850	T2m
ArchesWeather-M Couairon et al. [2024a]	1.5°	11.0	48.10	0.65	0.00054	1.29	1.34	**0.55**
NeuralGCM ENS (50) Kochkov et al. [2023]	1.4°	7680.0	**43.99**	0.66	0.00054	1.24	1.26	**0.55**
Stormer Nguyen et al. [2023]	1.4°	256.0	45.12	**0.61**	0.00053	1.14	1.16	0.57
AtmosMJ	1.5°	**5.7**	62.94	0.63	**0.00045**	**1.03**	**0.99**	0.70

4.3 Long-Term Forecast Stability and Physical Plausibility

Figure 4 presents the surface temperature simulation results at 850 hPa, specifically comparing the temperature distribution over the Antarctic region under different model configurations and prediction lead times. Panels (a) and (d) represent the "Ground Truth" (actual observed data) for January 1, 2020, and July 1, 2021, respectively. These two dates correspond to the Southern Hemisphere's summer and winter, clearly illustrating seasonal variations. The prediction results from AtmosMJ, which incorporates the Gated Residual Fusion (GRF) mechanism, are shown in

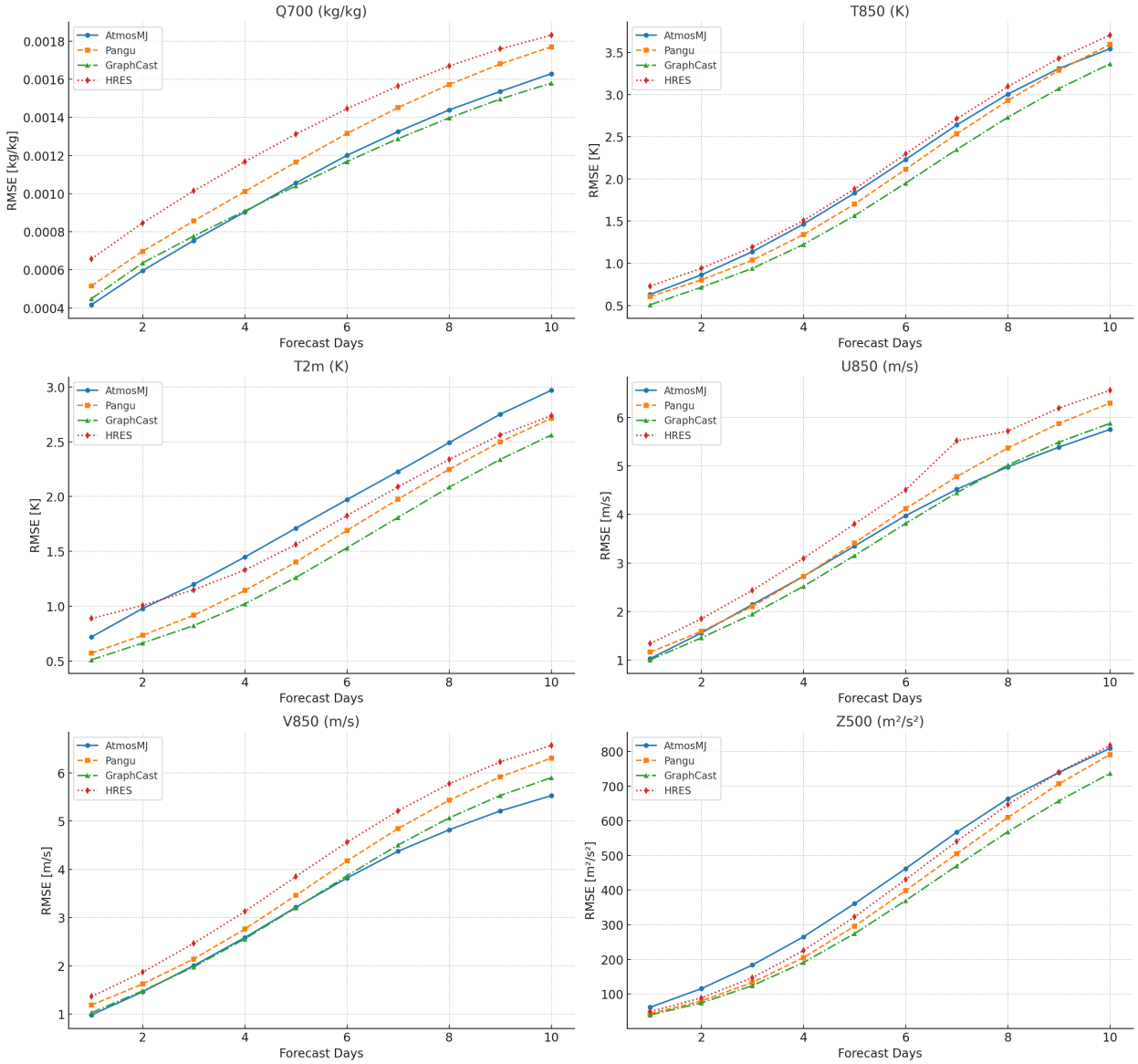

Figure 3: Global forecast performance of AtmosMJ versus state-of-the-art baselines. Latitude-weighted RMSE is shown for key variables over a 10-day horizon. Trained on lower-resolution data (1.5°), AtmosMJ matches Pangu-Weather and GraphCast, especially at longer lead times. For fairness, all baselines are evaluated at 1.5° using WeatherBench 2 deterministic scores.

panels (b) and (e). These panels represent long lead times of 730 and 1277 days, respectively. The AtmosMJ model could reproduce the observed temperature patterns and effectively capture seasonal variations. It accurately captures both the warm core and surrounding colder temperatures on January 1, 2020 (Southern Hemisphere summer), and the generally warmer Antarctic region on July 1, 2021 (Southern Hemisphere winter). This suggests that the AtmosMJ model effectively reflects seasonal changes even in long-term predictions. In contrast, panels (c) and (f) display the prediction results of the AtmosMJ model without the GRF mechanism ("wo_grf"), indicating the impact of GRF. These two panels yield a tendency for lower predicted temperatures; specifically, panel (c) is considerably colder than (b), and panel (f) remains overall colder compared to (e). This indicates that GRF influences the atmospheric temperature distribution, affecting both polar temperature prediction and the model's representation of seasonal changes.

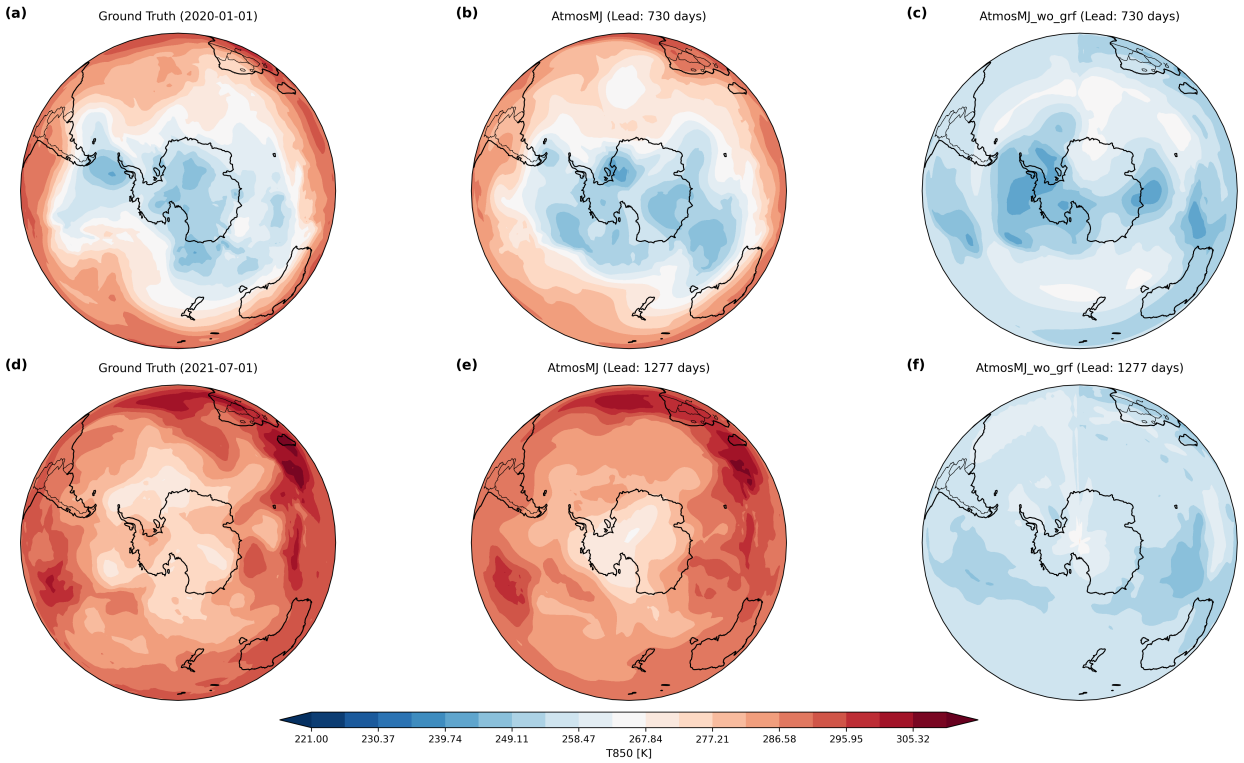

Figure 4: Surface temperature simulations at 850 hPa. Panels (a) and (d) show the ground truth on 2020-01-01 and 2021-07-01, respectively. Panels (b) and (e) display the AtmosMJ model output with lead times of 730 and 1277 days, respectively. Panels (c) and (f) show the AtmosMJ model without gravity wave drag (wo_grf) for the same lead times. The color bar indicates temperature in Kelvin.

Figure 5 provides a stark comparison of model performance after 397 autoregressive steps, contrasting the versions of AtmosMJ with and without the Gated Residual Fusion (GRF) module against the ERA5 ground truth. The leftmost panel, representing the model without GRF, shows a complete simulation collapse into a physically unrealistic state, demonstrating catastrophic error accumulation. In stark contrast, the main AtmosMJ model with GRF (center panel) produces a stable and physically plausible forecast that aligns closely with the ERA5 ground truth (right panel). The model faithfully reproduces key large-scale circulation features, such as the polar vortex over the Arctic and zonally elongated troughs over East Asia and North America. The trough associated with the Aleutian Low, for instance, is realistically captured in both shape and location. This direct comparison highlights that the GRF mechanism is critical for ensuring long-term stability and preventing numerical divergence in extended forecasts.

Furthermore, the proposed model can generate a full 500-day forecast in approximately 21 seconds on a single GPU, highlighting its potential for practical and rapid long-range simulation.

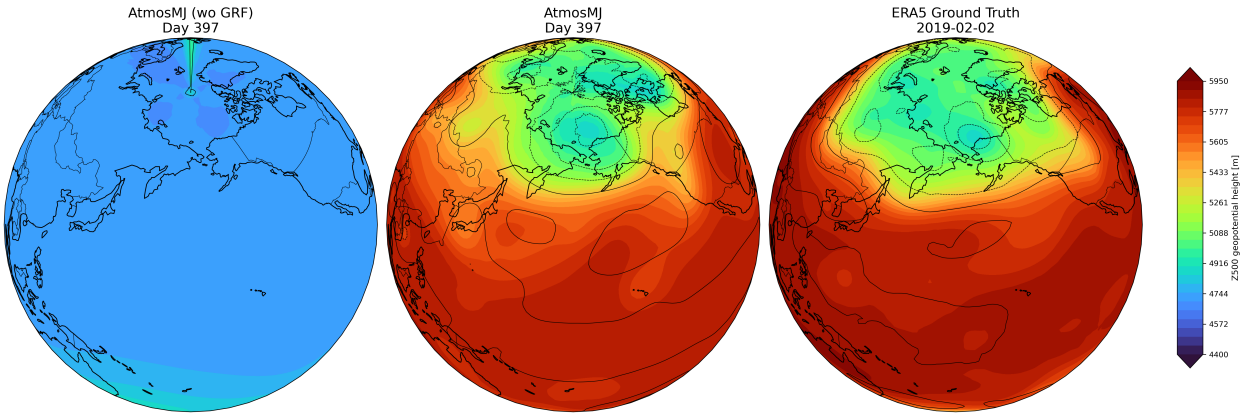

Figure 5: Comparison of 500 hPa geopotential height (Z500) and 1000 hPa height contours (Z1000) on simulation day 397 (2 February 2019). The figure compares forecasts from AtmosMJ without GRF (left) and with GRF (center) against the ERA5 ground truth (right).

As summarized in Table 4, our study highlights the feasibility of achieving long-term numerical stability directly on a conventional latitude–longitude grid. While prior models such as SFNO and DLWP-HPX relied on specialized coordinate systems (e.g., Spherical Harmonics and HEALPix) to produce stable forecasts beyond one year, AtmosMJ attains physically plausible forecasts for over 5 years without requiring any spatial transformation.

Table 4: Comparison of long-term forecasting models. AtmosMJ achieves year-scale stability without requiring specialized spatial transformations.

Model	**Grid Type**	**Stability**
SFNO Bonev et al. [2023]	Lat-Lon Grid (Spectral FFT)	1 year
DLWP-HPX Karlbauer et al. [2024]	HEALPix Mesh	1 year
AtmosMJ	Lat-Lon Grid	**5 years**

4.3.1 Analysis of Z500 Sensitivity

Figure 6 (bottom panel) presents the global mean Z500 over the same period. Similar to T2M, the ERA5 (black line) for Z500 also displays a distinct annual cycle, reflecting seasonal changes in the mid-tropospheric atmospheric structure and circulation. The AtmosMJ (hist) (red line) demonstrates excellent agreement with the ERA5 data, accurately replicating the amplitude and phase of the observed annual cycle in Z500. This concordance highlights the model's capability to simulate the seasonal variations in atmospheric height, which are intrinsically linked to thermal expansion and contraction of the atmosphere driven by solar energy. Conversely, the AtmosMJ (const) (green line) maintains a nearly constant 500 hPa geopotential height, hovering around 5500 m. This constant response, devoid of any annual periodicity, further underscores the critical role of dynamic solar forcing in accurately reproducing the seasonal variability of the middle atmosphere. The consistent deviation from the observed seasonal cycle by the constant TISR simulation emphasizes the necessity of incorporating realistic solar inputs for accurate atmospheric modeling. These results unequivocally establish the profound importance of accurate solar forcing for the realistic simulation of Earth's climate system, particularly its seasonal variability. The AtmosMJ model, when provided with the true historical values of TISR, successfully reproduces the observed annual cycles in both global mean T2M and Z500, demonstrating its robust capability to simulate fundamental atmospheric dynamics driven by solar energy. Conversely, fixing the TISR input leads to a complete failure in capturing these essential seasonal patterns.

5 Conclusion

This study set out to answer a central question in the development of AI-based weather models: whether transforming atmospheric data onto non-standard spatial domains is a prerequisite for achieving long-term forecasting stability. Through the development and evaluation of our model, AtmosMJ, we have demonstrated that this is not the case. By operating directly on the conventional latitude-longitude grid, our model successfully generated stable, physically

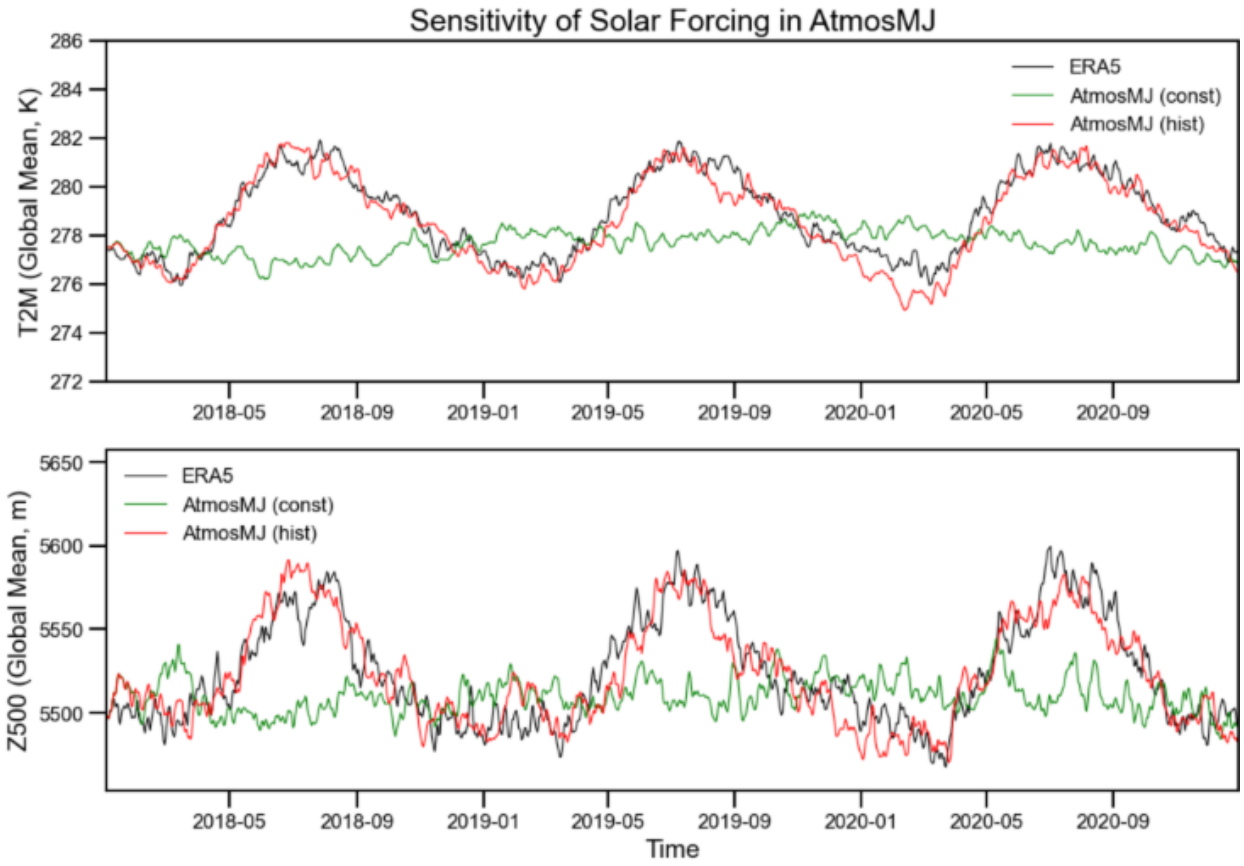

Figure 6: Sensitivity of Solar Forcing in AtmosMJ for T2M (top) and Z500 (bottom).

consistent forecasts for about 500 days, surpassing the year-long stability demonstrated by models reliant on specialized grids like spherical harmonics or HEALPix meshes.

Our primary contribution is the demonstration that architectural innovation can effectively replace the need for complex data transformations. The integration of the Gated Residual Fusion (GRF) mechanism proved critical in mitigating the long-term error accumulation that typically plagues autoregressive models, enabling a stable rollout far beyond the medium range. Qualitatively, AtmosMJ accurately captured key features of global circulation, including seasonal cycles and large-scale pressure systems, for the entire 500-day simulation. Quantitatively, it delivered competitive short-range forecast accuracy compared to existing models such as Pangu-Weather, GraphCast, and Stormer.

Remarkably, these results were achieved with exceptional computational efficiency, requiring only 5.7 V100-days for training. This significantly reduces the entry barrier for developing consistent long-range weather models. In conclusion, our work successfully decouples architectural design from data representation in the pursuit of long-term stability, highlighting a promising and more direct path toward building the next generation of efficient and accessible Large Weather Models.

Acknowledgements

The author would like to express sincere gratitude to Jeong-Hwan Kim, Seon-Yu Kang, Yo-Hwan Choi, CoG, CoS, and Marco Lee for their valuable discussions and unwavering moral support throughout the course of this research. In particular, Jeong-Hwan Kim, Seon-Yu Kang, and Yo-Hwan Choi have been deeply supportive since the author's development of the author's first AI weather model, KARINA, and their continued encouragement has been truly invaluable. Special thanks to CoL for carefully reviewing the manuscript.

References

Jay Chempan and contributors. Awesome lwms: A curated list of lightweight weather models. `https://github.com/jaychempan/Awesome-LWMs`, 2024. Accessed: 2025-06-08.

Kaifeng Bi, Lingxi Xie, Hengheng Zhang, Xin Chen, Xiaotao Gu, and Qi Tian. Accurate medium-range global weather forecasting with 3d neural networks. *Nature*, 619(7970):533–538, 2023.

Remi Lam, Alvaro Sanchez-Gonzalez, Matthew Willson, Peter Wirnsberger, Meire Fortunato, Ferran Alet, Suman Ravuri, Timo Ewalds, Zach Eaton-Rosen, Weihua Hu, et al. Graphcast: Learning skillful medium-range global weather forecasting. *arXiv preprint arXiv:2212.12794*, 2022.

Dmitrii Kochkov, Janni Yuval, Ian Langmore, Peter Norgaard, Jamie Smith, Griffin Mooers, Milan Klöwer, James Lottes, Stephan Rasp, Peter Düben, Sam Hatfield, Peter Battaglia, Alvaro Sanchez-Gonzalez, Matthew Willson, Michael P. Brenner, and Stephan Hoyer. Neural General Circulation Models for weather and climate. *arXiv preprint arXiv:2311.07222*, 2023.

Jaideep Pathak, Shashank Subramanian, Peter Harrington, Sanjeev Raja, Ashesh Chattopadhyay, Morteza Mardani, Thorsten Kurth, David Hall, Zongyi Li, Kamyar Azizzadenesheli, et al. Fourcastnet: A global data-driven high-resolution weather model using adaptive fourier neural operators. *arXiv preprint arXiv:2202.11214*, 2022.

Lei Chen, Xiaohui Zhong, Feng Zhang, Yuan Cheng, Yinghui Xu, Yuan Qi, and Hao Li. Fuxi: A cascade machine learning forecasting system for 15-day global weather forecast. *arXiv preprint arXiv:2306.12873*, 2023.

Tung Nguyen, Rohan Shah, Hritik Bansal, Troy Arcomano, Romit Maulik, Veerabhadra Kotamarthi, Ian Foster, Sandeep Madireddy, and Aditya Grover. Stormer: Scaling transformer neural networks for skillful and reliable medium-range weather forecasting. *arXiv preprint arXiv:2312.03876*, 2023.

Guillaume Couairon, Christian Lessig, Anastase A. Charantonis, and Claire Monteleoni. ArchesWeather: An efficient ai weather forecasting model at 1.5° resolution. *arXiv preprint arXiv:2405.14527*, 2024a.

Lei Chen, Xiaohui Zhong, Hao Li, Jie Wu, Bo Lu, Deliang Chen, Shang-Ping Xie, Libo Wu, Qingchen Chao, Chensen Lin, et al. A machine learning model that outperforms conventional global subseasonal forecast models. *Nature Communications*, 15(1):6425, 2024.

Boris Bonev, Thorsten Kurth, Christian Hundt, Jaideep Pathak, Maximilian Baust, Karthik Kashinath, and Anima Anandkumar. Spherical fourier neural operators: Learning stable dynamics on the sphere. *arXiv preprint arXiv:2306.03838*, 2023.

Matthias Karlbauer, Nathaniel Cresswell-Clay, Dale R. Durran, Raul A. Moreno, Thorsten Kurth, Boris Bonev, Noah Brenowitz, and Martin V. Butz. Advancing parsimonious deep learning weather prediction using the HEALPix mesh. *Journal of Advances in Modeling Earth Systems*, 16(8):e2023MS004021, 2024. doi:10.1029/2023MS004021.

Guillaume Couairon, Christian Lessig, Anastase Charantonis, and Claire Monteleoni. Archesweather: An efficient ai weather forecasting model at 1.5 {\deg} resolution. *arXiv preprint arXiv:2405.14527*, 2024b.

Stephan Rasp, Stephan Hoyer, Alexander Merose, Ian Langmore, Peter Battaglia, Tyler Russell, Alvaro Sanchez-Gonzalez, Vivian Yang, Rob Carver, Shreya Agrawal, et al. Weatherbench 2: A benchmark for the next generation of data-driven global weather models. *Journal of Advances in Modeling Earth Systems*, 16(6):e2023MS004019, 2024.

Weihao Yu, Pan Zhou, Shuicheng Yan, and Xinchao Wang. Inceptionnext: When inception meets convnext. In *Proceedings of the IEEE/cvf conference on computer vision and pattern recognition*, pages 5672–5683, 2024.

Minjong Cheon, Yo-Hwan Choi, Seon-Yu Kang, Yumi Choi, Jeong-Gil Lee, and Daehyun Kang. Karina: An efficient deep learning model for global weather forecast. *arXiv preprint arXiv:2403.10555*, 2024.

Junyoung Chung, Caglar Gulcehre, KyungHyun Cho, and Yoshua Bengio. Empirical evaluation of gated recurrent neural networks on sequence modeling. arxiv 2014. *arXiv preprint arXiv:1412.3555*, 1412, 2014.